

Article

One-Step Carbon Coating and Polyacrylamide Functionalization of Fe₃O₄ Nanoparticles for Enhancing Magnetic Adsorptive-Remediation of Heavy Metals

Mohamed A. Habila ^{1,*}, Zeid A. AlOthman ¹, Ahmed Mohamed El-Toni ^{2,3,*}, Joselito Puzon Labis ², Aslam Khan ², Adel Al-Marghany ¹ and Hussein Elsayed Elafifi ²

¹ Chemistry Department, College of Science, King Saud University, Riyadh-11451, Saudi Arabia; zaothman@ksu.edu.sa (Z.A.A.); amarghany@KSU.EDU.SA (A.A.-M.)

² King Abdullah Institute for Nanotechnology, King Saud University, Riyadh 11451, Saudi Arabia; jlabis@ksu.edu.sa (J.P.L.); aslamkhan@ksu.edu.sa (A.K.); helafifi@ksu.edu.sa (H.E.E.)

³ Central Metallurgical Research and Development Institute, CMRDI, Helwan, 11421 Cairo, Egypt

* Correspondence: mhabila@ksu.edu.sa (M.A.H.); aamohammad@ksu.edu.sa (A.M.E.-T.);

Tel: +966-1-4674-198 (M.A.H.); +966-1-4676-542 (A.M.E.-T.);

Fax: +966-1-4675-992 (M.A.H.); +966-1-4670-663 (A.M.E.-T.)

Received: 26 October 2017; Accepted: 23 November 2017; Published: 27 November 2017

Abstract: Magnetic nanoparticles are used in adsorptive removal of heavy metals from polluted wastewater. However, their poor stability in an acidic medium necessitates their protection with a coating layer. Coating magnetic nanoparticles with carbon showed proper protection but the heavy metal removal efficiency was slightly weak. However, to boost the removal efficiencies of surface functionalization, polyacrylamide was applied to carbon-coated Fe₃O₄ nanoparticles. In this paper, to facilitate the synthesis process, one-step carbon coating and polyacrylamide functionalization were conducted using the hydrothermal technique with the aim of enhancing the adsorptive removal capacity of Fe₃O₄ nanoparticles towards some heavy metals such as Cu(II), Ni(II), Co(II), and Cd(II). The results showed that the one-step process succeeded in developing a carbon coating layer and polyacrylamide functionality on Fe₃O₄ nanoparticles. The stability of the magnetic Fe₃O₄ nanoparticles as an adsorbent in an acidic medium was improved due to its resistance to the dissolution that was gained during carbon coating and surface functionalization with polyacrylamide. The adsorptive removal process was investigated in relation to various parameters such as pH, time of contact, metal ion concentrations, adsorbent dose, and temperature. The polyacrylamide functionalized Fe₃O₄ showed an improvement in the adsorption capacity as compared with the unfunctionalized one. The conditions for superior adsorption were obtained at pH 6; time of contact, 90 min; metal solution concentration, 200 mg/L; adsorbent dose, 0.3 g/L. The modeling of the adsorption data was found to be consistent with the pseudo-second-order kinetic model, which suggests a fast adsorption process. However, the equilibrium data modeling was consistent with both the Langmuir and Freundlich isotherms. Furthermore, the thermodynamic parameters of the adsorptive removal process, including ΔG° , ΔH° , and ΔS° , indicated a spontaneous and endothermic sorption process. The developed adsorbent can be utilized further for industrial-based applications.

Keywords: adsorption; water treatment; magnetic separation; nanotechnology; solvothermal technique; heavy metals

1. Introduction

Water contamination with heavy metals is a source of concern since the metal cations tend to accumulate within the environment [1]. Rain and snow can wash toxic metal elements into lakes, reservoirs, and underground water. Cadmium, nickel, copper, cobalt, etc. exist in industrial wastewater and upon transfer to water streams can lead to bioaccumulation in living systems that can cause health issues in animals and humans such as cancer or kidney failure [3,4]. Therefore, improvement of the adsorbents for higher adsorption ability for removal of metal cation pollution from water is required and considered a priority research topic. The traditional methods for metal pollution remediation include chemical precipitation, electro-flotation, ion exchange, reverse osmosis, and adsorption, which is the recommended method [5–13]. Nanostructure adsorbents have exhibited much higher efficiency and faster adsorption rates in water treatment when compared to traditional ones [14,15]. However, the main drawbacks of nanostructure adsorbents are the difficulty of their separation. Magnetic nanomaterials can be easily and rapidly separated from an aqueous solution under an external magnetic field due to their features of simplicity, efficiency, and sensitivity [16–21].

The enhancement of the adsorptive removal capacity of magnetic nanoparticles can be done either by surface functionalization or by improving the chemical stability [22–27]. Usually, adsorption of heavy metal cations takes place in an acidic medium, while Fe_3O_4 is not stable in this condition. Therefore, it is necessary to protect Fe_3O_4 nanoparticles by surface coating to make them stable in this environment. Carbon coating was applied to protect magnetic nanoparticles within an acidic medium and the carbon layer was also utilized for adsorptive removal of heavy metals. Additionally, a protective coating layer was implemented together with attaching some functional groups to improve their adsorption efficiency [28]. Tang et al. (2012) synthesized Fe_3O_4 @mesoporous silica composite microspheres (MS) and polyethylenimine (PEI) functionalization of Fe_3O_4 @mesoporous silica composite microspheres by solvothermal reaction for humic acid adsorption [29], where the silica shell acted as a protective coating and PEI was the surface functional moiety. Tang et al. (2013) prepared amino-functionalized Fe_3O_4 @mesoporous SiO_2 core-shell composite microspheres for Pb(II) and Cd(II) adsorption and silica worked as a protective layer with immobilized amino groups to chelate heavy metal cations [30]. However, most of these reports implemented two-step synthesis processes where in the first step was to develop a protective coating layer and the second was to impart a functional group. Therefore, this work aims to facilitate the synthesis process through developing one-step carbon coating and polyacrylamide functionalization using a hydrothermal technique to enhance the adsorptive removal capacity of Fe_3O_4 nanoparticles towards some heavy metals, such as Cu(II), Ni(II), Co(II), and Cd(II). Factors controlling the adsorption of these heavy metals such as pH, time of contact, and concentration of metal ion solutions were optimized. Different kinetic models, isotherms, and thermodynamic equations were applied to the adsorption data.

2. Results and Discussion

2.1. Properties of the Fabricated Polyacrylamide Functionalized Magnetic Nanoparticles

The application of the adsorption process for heavy metal removal depends mainly on the surface functional groups of the adsorbent and their morphology. Therefore, the fabricated polyacrylamide-functionalized magnetic nanoparticles were characterized by SEM, TEM, XRD, and FTIR. The SEM image showed the rough surface morphology of the particle which contains some cavities (Figure 1A). TEM image (Figure 1B) showed that the magnetic nanoparticles were uniform, with an average particle size of around 50–70 nm. The magnetic nanoparticles were impeded within the carbon matrix formed by carbonization of glucose molecules under the hydrothermal condition. Moreover, the magnetic Fe_3O_4 nanoparticles were evenly and homogeneously distributed within the carbon matrix.

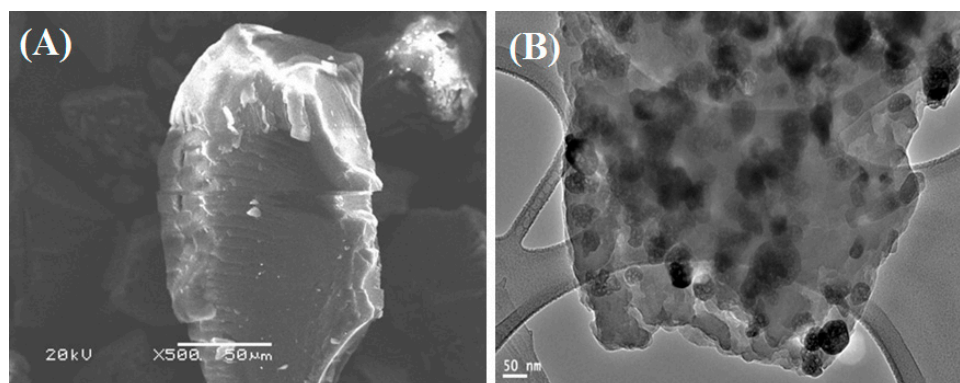


Figure 1. (A) SEM and (B) TEM of polyacrylamide functionalized Fe_3O_4 nanoparticles.

To investigate the crystalline character of Fe_3O_4 nanoparticles before and after surface functionalization, X-ray diffraction spectra for bare and polyacrylamide functionalized Fe_3O_4 nanoparticles were conducted, as shown in Figure 2A. The X-ray diffraction pattern for the bare Fe_3O_4 showed the existence of six peaks that matched well with the pure magnetite phase ((220), (311), (400), (511), and (440) planes of fcc structured Fe_3O_4 (JCPDS, 85-1436)), which suggests the presence of a cubic crystal system [31]. Upon performing surface functionalization using polyacrylamide, the X-ray diffraction pattern did not show any noticeable changes at the peaks, which suggests the maintaining of the Fe_3O_4 cubic phase. However, there was a slight reduction in the peak intensity that can be attributed to the shielding effect of the polyacrylamide matrix [32,33]. In order to examine the surface functionality of the synthesized polyacrylamide functionalized Fe_3O_4 nanoparticles, FTIR measurements were carried out for the bare and polyacrylamide functionalized Fe_3O_4 nanoparticles, displayed in Figure 2B. The FTIR spectra of the bare Fe_3O_4 sample showed a peak at 585 cm^{-1} , which is due to Fe–O bonding vibration, while the peak appearing at 3420 cm^{-1} arose from OH⁻ adsorbed on the Fe_3O_4 nanoparticles. However, after functionalization of Fe_3O_4 with polyacrylamide, the peak characteristic for Fe–O bonding at 570 cm^{-1} was suppressed, which can be attributed to the shielding effect of the polyacrylamide layer [32,33]. The main functional group of polyacrylamide (amide I and amide II) appeared as a broad band ($1580\text{--}1700\text{ cm}^{-1}$), which also interfered with the OH functional group that existed in the same range. The amide II group that refers to the bending vibration of NH₂ was noticed at 1620 cm^{-1} , while the amide I group that refers to C=O bonding existed at 1680 cm^{-1} . Moreover, the third functional group of polyacrylamide was observed at 1430 cm^{-1} for stretching vibration of C–N bonding. Additionally, a broad peak from $3300\text{--}3600\text{ cm}^{-1}$ was observed, which is related to the combination of the peaks of NH and OH.

To evaluate the stability of Fe_3O_4 in an acidic medium after functionalization with polyacrylamide, bare and polyacrylamide functionalized Fe_3O_4 nanoparticles were soaked in 0.1 M HCl and the results are shown in Figure S1 (see Supplementary Materials). The results represent the dissolution percentage in the case of bare Fe_3O_4 , which was considered to be 100% compared with 20% in the case of polyacrylamide functionalized Fe_3O_4 . This means that polyacrylamide functionalized Fe_3O_4 was stable and protected from dissolution in an acidic medium, making it more proper for heavy metal adsorption, which usually occurs in an acidic medium.

To elucidate the effect of the carbon coating as well as polyacrylamide functionalization on the magnetic character of Fe_3O_4 , the magnetic property was measured for the bare Fe_3O_4 and polyacrylamide-functionalized Fe_3O_4 as shown in Figure 3A. It is clear that Fe_3O_4 showed high magnetic strength with a saturated magnetization of $67\text{ emu}\cdot\text{g}^{-1}$. After performing carbon coating and polyacrylamide functionalization, there was a noticeable reduction in the magnetic strength to reach saturated magnetization of $31\text{ emu}\cdot\text{g}^{-1}$. However, after such reduction in magnetic strength, polyacrylamide-functionalized Fe_3O_4 can still be easily separated from the solution under the effect of the external magnetic field. The textural properties, specific surface area, and total pore volume were also evaluated for polyacrylamide-functionalized Fe_3O_4 through performing the N₂ sorption isotherm, which is displayed in Figure 3B. It can be seen that the isotherm possessed type IV, which may be due to the non-ordered pores and cavities within the polyacrylamide-functionalized

carbon-coated Fe₃O₄ matrix. The specific surface area of 8.225 m²/g and total pore volume of 0.015 cc/g are indicative of weak textural properties and suggest their limited contribution to the adsorptive removal of heavy metal cations.

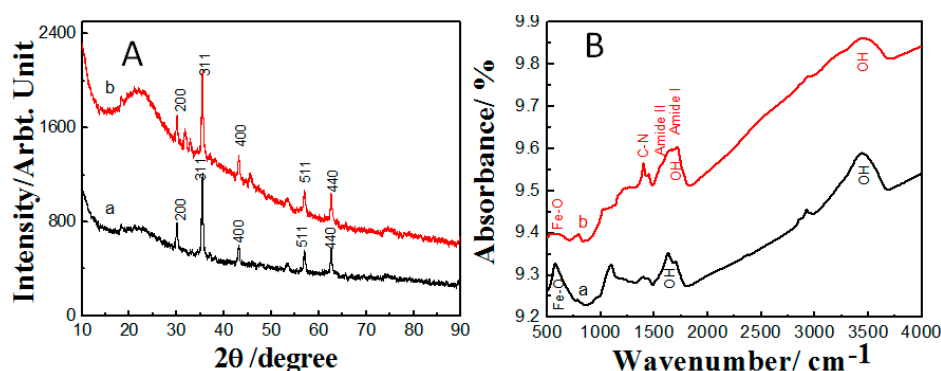


Figure 2. (A) XRD patterns and (B) FTIR spectra of (a) bare Fe₃O₄ and (b) polyacrylamide functionalized Fe₃O₄ nanoparticles.

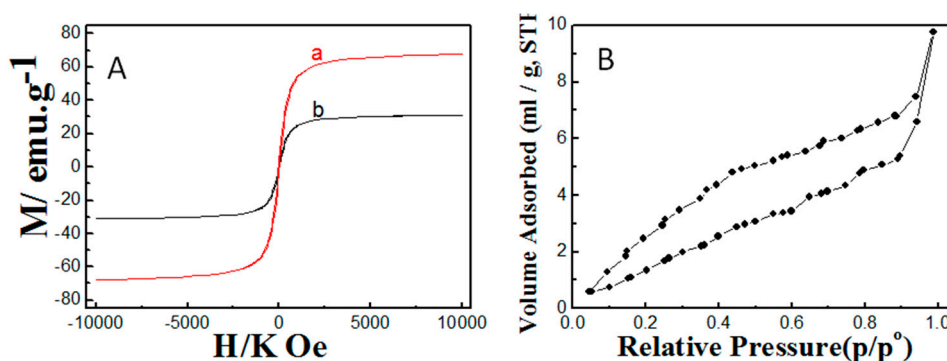


Figure 3. (A) Magnetic strength of (a) bare Fe₃O₄ and (b) polyacrylamide functionalized Fe₃O₄; (B) nitrogen sorption of polyacrylamide functionalized Fe₃O₄ nanoparticles.

2.2. Adsorption Characteristics

2.2.1. Effect of pH and Concentration of Heavy Metal Solution

The adsorption process is significantly affected by the pH of metal cations in an aqueous solution. Controlling the pH or concentration of hydrogen ions could replace the metal cations on the active sites of adsorbent surface and finally impact the ionization behavior of metal cations during the adsorption process [25]. The effects of pH on heavy metal cations adsorption at an initial concentration of 100, 200, and 300 mg/L for the abovementioned metal cations are shown in Figure 4. Additionally, Fe₃O₄ is applied as an adsorbent at a metal concentration of 200 mg/L, where the obtained adsorption capacity was quite low compared with polyacrylamide modified Fe₃O₄ (Figure 4). At low pH values (<4), the adsorption capacities of Cu(II), Ni(II), Co(II), and Cd(II) on polyacrylamide functionalized Fe₃O₄ were low, while at higher pH values (4 to 7) the adsorption capacities showed much higher values. However, the maximum adsorption capacity was obtained at a pH of 6. The acidic medium is reported to allow high efficiency for heavy metals' adsorptive removal due to the competition between H⁺ and heavy metals for the binding sites of polyacrylamide functionalized Fe₃O₄, resulting in a decrease in their adsorption capacity in the strongly acidic medium [25]. Furthermore, amide groups in the polyacrylamide-functionalized magnetic nanoparticles are protonized at a low pH, which results in the passivation of adsorption sites and hence reduces the metal adsorption capacities. These results are in agreement with the findings of Ayub et al. and Hashem et al., who reported that heavy metal cations are completely released from adsorption sites under strongly acid conditions [34,35]. Upon increasing the concentration of heavy metal from 100 mg/L to 200 mg/L, it can be noticed that the adsorption

capacity has been promoted for heavy metal cations. However, there is no significant change of adsorption behavior when elevating the concentration of heavy metal from 200 mg/L to 300 mg/L. For comparison purposes, the activated carbon adsorption capacity was tested for the removal of heavy metal cations of 200 mg/L concentrations at the same conditions. The results shown in Figure 4 indicate that activated carbon without any modification has a poor adsorption capacity for heavy metals as compared to the polyacrylamide functionalized Fe_3O_4 .

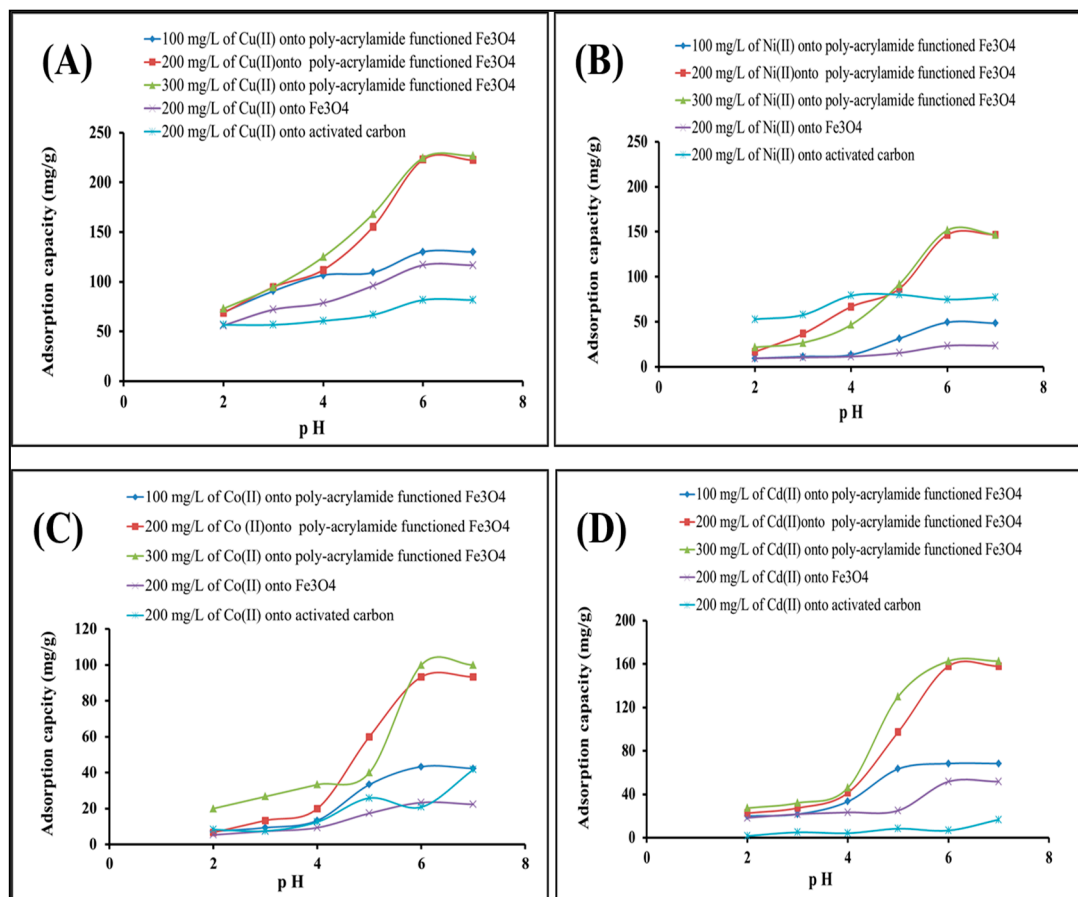


Figure 4. Effect of pH of (A) Cu(II); (B) Ni(II); (C) Co(II); and (D) Cd(II) on adsorption capacity upon mixing 0.5 g/L activated carbon with 200 mg/L of a metal cation solution, 0.5 g/L Fe_3O_4 nanoparticles, and 0.5 g/L polyacrylamide functionalized Fe_3O_4 nanoparticles with 100, 200, and 300 mg/L solutions of metal cations and 25 °C.

2.2.2. Kinetics of Adsorption

The rate of the adsorption process was predicted by examining kinetic parameters. In order to elucidate adsorption process kinetics, the time needed to attain the equilibrium as well as the highest heavy metal adsorption should be addressed. The change in concentration of heavy metals in the adsorption mixture was observed by measuring the decrease in the heavy metal concentration overtime. In this regard, the time of contact of polyacrylamide functionalized magnetic nanoparticles with a solution containing heavy metals varied in the range of 10–120 min. The time of contact optimization results are displayed in Figure 5. It can be seen that heavy metals were rapidly adsorbed onto the surface of polyacrylamide functionalized Fe_3O_4 within 90 min. However, contact was continued for up to four hours to confirm the achievement of equilibrium status. The adsorption behavior differs from one element to another; the Cu cations showed the maximum adsorption capacity, while Co showed much less. The time of contact results suggest that 90 min was adequate to accomplish equilibrium. From Figure 5, the adsorption capacity did not change effectively with further increments in the time of contact. At 90 min, the adsorption capacity was recorded at 194,

144.3, 128, and 161 mg/g for Cu(II), Ni(II), Co(II), and Cd(II), respectively, which are considered the maximum adsorption capacities.

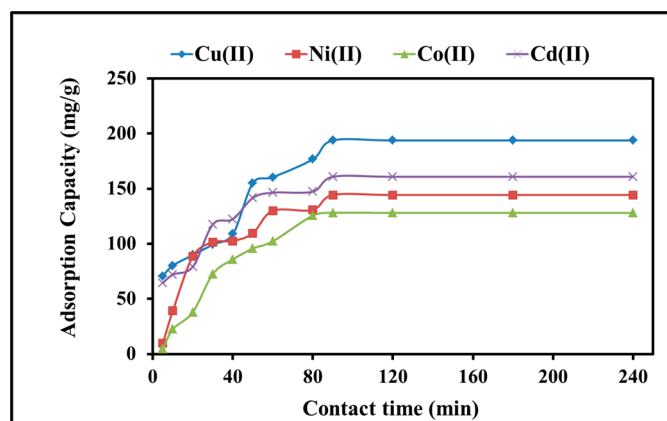


Figure 5. Effect of time of contact of heavy metal cations on the adsorption capacity upon mixing 0.3 g/L polyacrylamide functionalized Fe₃O₄ nanoparticles with 150 mg/L metal cations solution at pH 6 and 25 °C.

The pseudo-first-order equation of Lagergren, as described by Wen et al. was applied to the adsorption of heavy metal cations onto 0.3 g/L polyacrylamide functionalized Fe₃O₄ nanoparticles at pH 6, and 25 °C. The equation is generally expressed in the integrated form of Equation (1) [36]:

$$\log(q_e - q_t) = \log q_e - k_1 t / 2.303 \quad (1)$$

The pseudo-first-order rate constant, k_1 , was calculated from the slope of the graph of $\log(q_e - q)$ versus time t (Figure 6A). The calculated k_1 values and corresponding linear regression correlation coefficient values are shown in Table 1. It is clear that the linear regression correlation coefficient value R^2 was no more than 0.93 and the calculated q_e values (239.8, 128.8, 208.9, and 114.8 mg/g) were significantly different from the experimental q_e ones (194, 144.3, 128, and 161 mg/g) for Cu(II), Ni(II), Co(II), and Cd(II), respectively. The results indicate that the pseudo-first-order model cannot be applied to predict the adsorption kinetics.

In addition, the pseudo-second-order kinetic rate equation was applied to the obtained adsorption capacities to evaluate their fittingness. The equation is expressed in the integrated form of Equation (2) [37]:

$$t/q_t = 1/Kq_e^2 + 1/q_e t \quad (2)$$

where t refers to the time of contact (min), and q_e (mg/g) and q_e^2 (mg/g) refer to the amount of solute adsorbed at equilibrium for adsorption of heavy metal cations onto 0.3 g/L polyacrylamide-functionalized Fe₃O₄ nanoparticles at pH 6 and 25 °C. Figure 6B shows the linear relationship of the graph plot of t/q_t versus t , from which q_e and k can be determined from the slope and intercept, respectively.

The calculated k_2 values and corresponding linear regression correlation coefficient values are shown in Table 2. Results showed that the calculated q_e values (200.18, 150.7, 130.6, and 167.7 mg/g) more closely fit the experimental q_e data (194, 144.3, 128, and 161 mg/g) for Cu(II), Ni(II), Co(II), and Cd(II), respectively. Moreover, the model fitting was much better than for the pseudo-first-order one. According to these results, it can be said that the pseudo-second-order kinetic model provided a good correlation for the description of the mechanism of sorption of heavy metals onto polyacrylamide functionalized Fe₃O₄ nanoparticles. From these results, it can be concluded that the adsorption process is fast and the rate of the reaction is mainly controlled by migration of the metal ions from solution to the surface of the adsorbent and migration of the metal ions to the pores of the adsorbent [38,39].

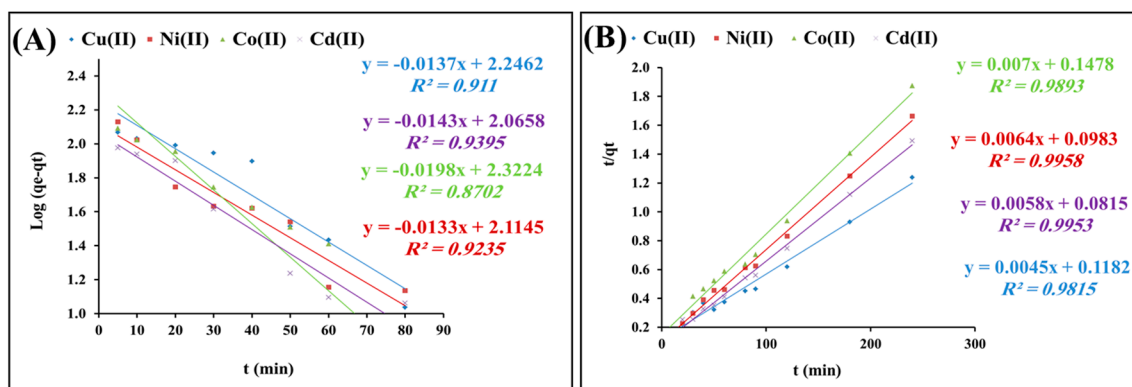


Figure 6. Pseudo-first-order (A) and pseudo-second-order; (B) of heavy metal adsorption tests upon mixing 0.3 g/L polyacrylamide functionalized Fe_3O_4 nanoparticles with 150 mg/L metal cations solution at pH 6 and 25 °C.

Table 1. Kinetic constant parameters obtained for adsorption of heavy metal onto polyacrylamide functionalized Fe_3O_4 nanoparticles.

	Pseudo-First-Order				Pseudo-Second-Order			
	$q_e, \text{exp (mg/g)}$	$K_1 (\text{min}^{-1})$	$q_e, \text{cal (mg/g)}$	R^2	$k_2 (\text{g/mg}\cdot\text{min})$	$q_e, \text{cal (mg/g)}$	R^2	
Cu(II)	194	0.031	239.8	0.91	5.7×10^{-4}	200.18	0.98	
Ni(II)	144.3	0.030	128.8	0.92	6.8×10^{-4}	150.7	0.99	
Co(II)	128	0.045	208.9	0.87	12.8×10^{-4}	130.6	0.98	
Cd(II)	161	0.035	114.8	0.93	6.8×10^{-4}	167.7	0.99	

2.2.3. Effect of Adsorbent Dose

To identify the proper adsorbent dose to reach optimum adsorption process, various amounts of polyacrylamide functionalized Fe_3O_4 nanoparticles were mixed with heavy metal solutions; the results are presented in Figure 7. The adsorption capacity of Cu(II), Ni(II), Co(II), and Cd(II) decreased from 181.9, 130.5, 113.8, and 145.8 mg/g to 22.9, 16.1, 16.7, and 22.0 mg/g, respectively, upon elevating the adsorbent concentration from 0.3 to 1.5 g/L for an initial metal concentration of 140 mg/L at pH 6. Such behavior is expected since at a low adsorbent dosage it will be saturated with heavy metal species and the adsorption capacity reaches its maximum value. However, when increasing the dosage gradually, there will be many active adsorption sites that will not interact with the adsorbate species. Hence, there will be a reduction in the calculated adsorption capacity under these conditions.

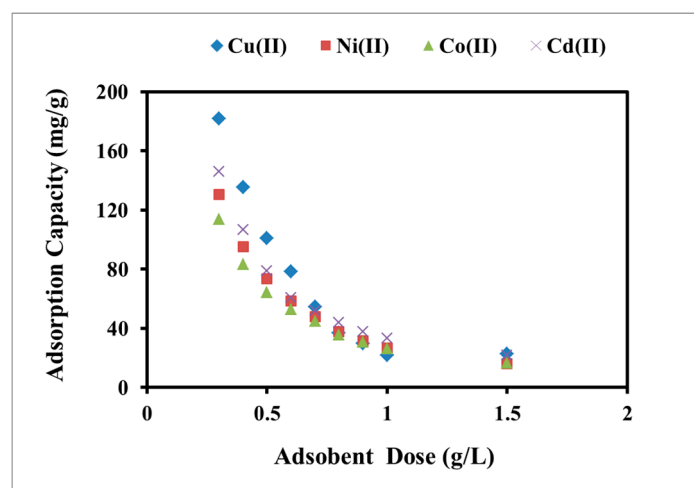


Figure 7. Effect of polyacrylamide functionalized Fe_3O_4 nanoparticles dose on the adsorption capacity of heavy metal cations at pH 6, contact time of 90 min, 140 mg/L of metal, and 25 °C.

2.2.4. Isotherms Study

Studying the adsorption isotherms is crucial to identifying the distribution process of adsorbate molecules within the liquid and solid phases at the equilibrium state of adsorption process [40]. Figure 8A,B shows the adsorption isotherms for heavy metal onto polyacrylamide functionalized Fe₃O₄ nanoparticles at 25 °C and pH 6. The Langmuir equation (Equation (3)) was applied to the equilibrium adsorption data for heavy metal cations onto polyacrylamide functionalized Fe₃O₄ nanoparticles [41]:

$$C_e/Q_e = 1/(q_{max} \cdot b) + C_e/q_{max} \quad (3)$$

Where C_e refers to the equilibrium concentration of the adsorbate (mg/L), Q_e refers to the amount of metal ion adsorbed (mg/g), and q_{max} and b refer to Langmuir constants, which are related to the maximum adsorption capacity (mg/g) and the adsorption energy, respectively. The Langmuir equilibrium constant, K_L , can be obtained from Equation (4):

$$K_L = q_{max} \cdot b \quad (4)$$

The linear form of the Langmuir isotherm is shown in Figure 8A. The correlation coefficient, R^2 , for the adsorption of heavy metal onto polyacrylamide functionalized Fe₃O₄ nanoparticles, is 0.0.92, 0.95, 0.97, and 0.91, respectively, indicating that the adsorption parameters were well fitted by the Langmuir isotherm. These results suggest that the maximum adsorption capacity corresponds to saturated monolayer coverage of heavy metal onto polyacrylamide functionalized Fe₃O₄ nanoparticles, which means that the energy of the adsorption process is constant, with a low possibility of transmigration.

Contrary to the Langmuir isotherm, which assumes the formation of a monolayer of adsorbate onto the adsorbent, the Freundlich isotherm postulates the formation of multiple layers of adsorbate molecules onto the surface of adsorbent material. The obtained data for adsorption of heavy metal onto polyacrylamide functionalized Fe₃O₄ nanoparticles were investigated using the Freundlich equation (Equation (5)):

$$\log q_e = \log K_f + 1/n \log C_e \quad (5)$$

Where C_e refers to the equilibrium concentration (mg/L) and q_e refers to the amount of metal adsorbed (mg/g) at equilibrium. The quantities K_F and n refer to the Freundlich constants, with K_F (mg/g) referring to the adsorbent capacity and n referring to the favorable nature of the process. Plots of $\log q_e$ versus $\log C_e$ give the slope and intercept of the line obtained corresponding to $1/n$ and $\log K_F$, respectively (Figure 8B).

The calculated results of the Langmuir and Freundlich isotherm constants are given in Table 2. The adsorption of heavy metal onto polyacrylamide modified Fe₃O₄ nanoparticles showed good correlation with the Langmuir and Freundlich equations ($R^2 > 0.9$) for the range of concentrations used in this study, which could suggest that the adsorption process of heavy metal onto polyacrylamide modified Fe₃O₄ nanoparticles involved both mono- and multilayer behavior.

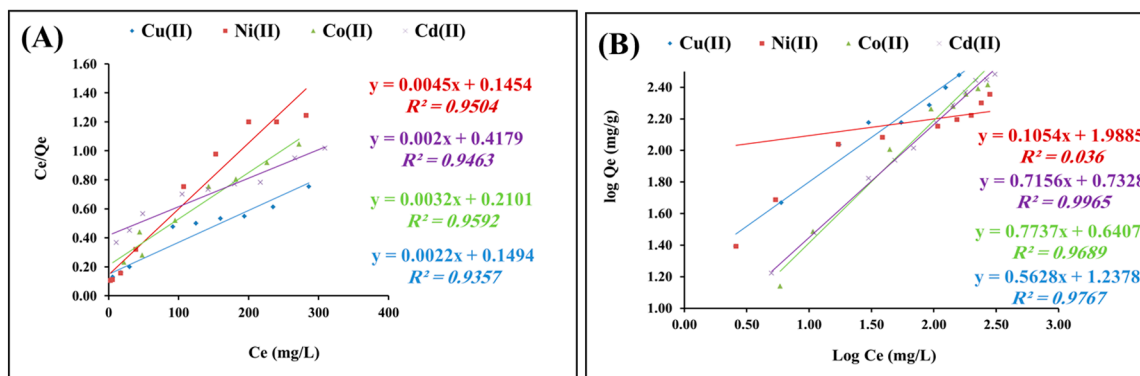


Figure 8. (A) Langmuir and (B) Freundlich isotherms for adsorption of heavy metal cations onto polyacrylamide functionalized Fe₃O₄ nanoparticles.

Table 2. Langmuir and Freundlich constants for the adsorption of Cu(II), Ni(II), Co(II), and Cd(II) onto polyacrylamide functionalized Fe₃O₄ nanoparticles.

	Langmuir Constants				Freundlich Constants		
	K _L	b	Q _{max}	R ²	K _F	n	R ²
Cu(II)	5.9	0.013	454.5	0.92	17.4	1.78	0.97
Ni(II)	6.9	0.031	222.2	0.95	22.6	2.42	0.92
Co(II)	4.7	0.015	312.5	0.97	5.09	1.38	0.96
Cd(II)	2.3	0.0043	526.3	0.91	5.42	1.39	0.99

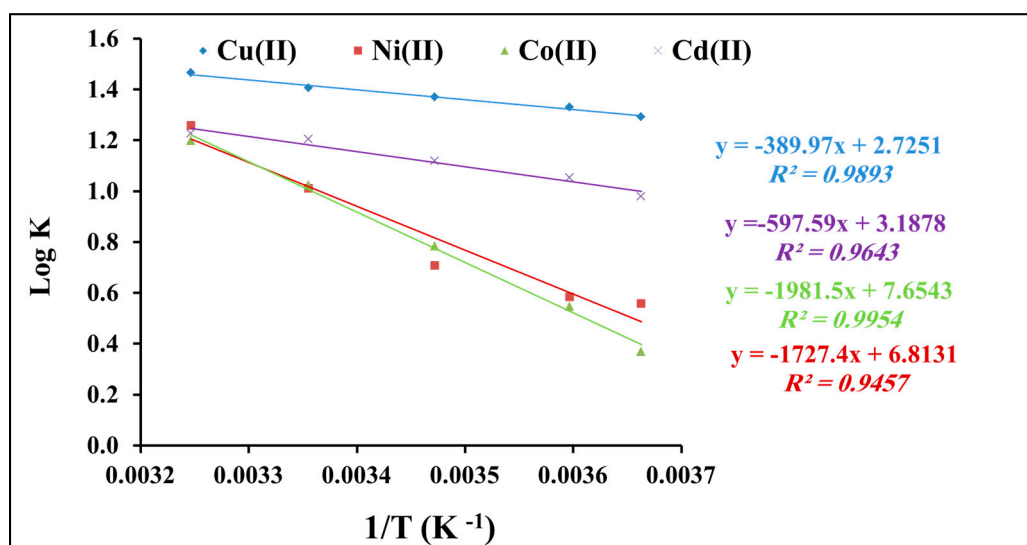
2.2.5. Thermodynamic Studies

The Gibbs free energy (ΔG°), enthalpy (ΔH°), and entropy (ΔS°) of the heavy metal uptake onto polyacrylamide functionalized Fe₃O₄ nanoparticle are evaluated to explain the sorption process. They are calculated using Equations (6) and (7):

$$\log K_d = \Delta S^\circ / 2.303R - \Delta H^\circ / 2.303RT \quad (6)$$

$$\Delta G^\circ = -RT \ln K_d \quad (7)$$

where K_d refers to the equilibrium partition constant calculated based on the ratio between sorption capacity (q_e) and equilibrium concentration (C_e) for heavy metal uptake onto polyacrylamide-functionalized Fe₃O₄ nanoparticles at pH 6, R refers to the gas constant (8.314 J/mol K), and T refers to the temperature in Kelvin (K). From Equation (9), by plotting $\log K_d$ vs. $1/T$ (Figure 9), ΔH° and ΔS° values can be obtained.

**Figure 9.** Thermodynamic factors for the adsorption of heavy metal cations onto polyacrylamide functionalized Fe₃O₄ nanoparticles.

The values of Gibbs free energy (ΔG°), enthalpy (ΔH°), and entropy (ΔS°) are shown in Table 3. ΔG° was in the range (−6.8 to −8.6 kJ/mol) for Cu(II), (−2.9 to −7.4 kJ/mol) for Ni(II), (−1.9 to −7.1 kJ/mol) for Co(II), and (−5.1 to −7.2 kJ/mol) for Cd(II). ΔH° and ΔS° values were in the range of 52.2 to 146.6 kJ·mol^{−1} and 7.5 to 37.9 J mol^{−1} K^{−1}, respectively.

These values suggest the following characteristics: (i) the adsorption of heavy metal onto polyacrylamide functionalized Fe₃O₄ nanoparticles was spontaneous; (ii) the adsorption process is a typical physical process with an endothermic nature; and (iii) the process is accompanied by an increase in the degree of freedom of the adsorbed species [42,43].

Table 3. Thermodynamic parameters for adsorption of heavy metal cations onto polyacrylamide functionalized Fe₃O₄ nanoparticles.

	Temperature T(K)	Thermodynamic Parameters		
		ΔG° (kJ/mol)	ΔS° (J/mol/K)	ΔH° (kJ/mol)
Cu(II)	273	-6.8	52.2	7.5
	278	-7.1		
	288	-7.6		
	298	-8.0		
	308	-8.6		
Ni(II)	273	-2.9	130.5	33.1
	278	-3.1		
	288	-3.9		
	298	-5.8		
	308	-7.4		
Co(II)	273	-1.9	146.6	37.9
	278	-2.9		
	288	-4.3		
	298	-5.8		
	308	-7.1		
Cd(II)	273	-5.1	61.0	11.4
	278	-5.6		
	288	-6.2		
	298	-6.9		
	308	-7.2		

2.2.6. Quality Control Assessment

In order to investigate the repeatability of the results and the quality control assessment, an experiment composed of three replicate treatments for the effect of the heavy metal concentration on the adsorption capacity was conducted. Results are presented in Table 4. The results show high repeatability of the adsorption capacity for the treatment process for the tested metal ions in the concentration range of 50 mg/L to 250 mg/L. At the same time, the blank experiments that were conducted simultaneously did not show any removal behavior for heavy metal cations, indicating the effectiveness of the prepared absorbent.

Table 4. Impact of heavy metal concentration on the adsorption capacity ($n=3$).

Metal ion Concentration (ppm)	Adsorption Capacity ($Q_e \pm SD$)			
	Cu	Ni	Co	Cd
50	105.1 ± 4.5	105.3 ± 3.5	88.1 ± 5.5	74.4 ± 6.9
100	156.7 ± 6.7	132.2 ± 1.9	180.9 ± 7.2	104.4 ± 5.1
150	192.2 ± 1.9	144.1 ± 2.3	184.4 ± 1.9	156.7 ± 6.7
200	250.0 ± 3.3	153.3 ± 5.8	186.7 ± 5.8	187.8 ± 5.1
250	301.7 ± 2.4	170.0 ± 4.7	230.0 ± 2.4	231.7 ± 2.4

3. Experimental Section

3.1. Synthesis and Characterization of Fe₃O₄ Nanoparticles and Polyacrylamide Functionalized Fe₃O₄

Chemicals including ferric chloride hexahydrate (FeCl₃·6H₂O), sodium acetate, sodium citrate, polyacrylamide, and glucose were obtained from Sigma-Aldrich (St. Louis, MO, USA). For synthesis of Fe₃O₄ nanoparticles, a precise amount of sodium acetate and FeCl₃·6H₂O were added to a specific volume of ethylene glycol. The mixture solution was stirred until homogeneity was achieved. Then the mixture solution was charged in a Teflon-coated stainless-steel autoclave and heated to 180 °C for 12 h. Then the autoclave was left to cool down to room temperature. The produced nanoparticles were washed with ethanol and de-ionized water for three times and then redispersed in de-ionized water.

One-step carbon coating and polyacrylamide surface functionalization of magnetic Fe₃O₄ nanoparticles were executed by means of a hydrothermal reaction. A known weight (0.05 g) of the previously synthesized Fe₃O₄ nanoparticles was dispersed in a known volume of 0.5 M glucose solution and thereafter a specific amount of polyacrylamide (0.5 g) was introduced to the mixture solution. The mixture was loaded in a Teflon-coated stainless-steel autoclave and heated at 200 °C for 3 h. The produced carbon-coated and polyacrylamide functionalized Fe₃O₄ nanoparticles were washed with ethanol and deionized water three times [15]. However, for ease, the produced material will be described as “polyacrylamide functionalized Fe₃O₄”. A scanning electron microscope (JSM-7600F, JEOL, Tokyo, Japan) was utilized to obtain the sample morphology. Transmission electron microscopy (TEM) characterization was conducted to study the carbon coating and dispersity of magnetic Fe₃O₄ nanoparticles using a JEM-2100F electron microscope, Tokyo, Japan. Powder X-ray diffraction (XRD) measurements were conducted using X’Pert PRO MPD, PANalytical, Almelo, The Netherlands) on bare and carbon-coated polyacrylamide functionalized samples to investigate the crystalline character of the samples. To elucidate the functionality after carbon coating and the functionalization step, Fourier transform infrared (FTIR) spectra were recorded using a Vertex-80 spectrometer (Bruker, Billerica, MA, USA).

3.2. Adsorptive Removal of Heavy Metal Ions on Polyacrylamide Functionalized Fe₃O₄

Batch procedures were used to study the adsorption of heavy metal cations on polyacrylamide functionalized Fe₃O₄ in term of kinetics and thermodynamics, as described in Wang et al. [44]. Stalk metals solution (300 mg/L) were prepared from nitrate salts, which were bought from Sigma-Aldrich. The other metal concentrations (100 mg/L and 200 mg/L) were prepared by dilution. Ten milliliters of multi-metal cation Cu(II), Ni(II), Co(II), and Cd(II) solution were mixed with 0.01 g of polyacrylamide modified Fe₃O₄ in Erlenmeyer flasks. The mixture was subjected to shaking at a speed of 150 rpm for a desired time. By the completion of the adsorption test, the adsorbent was separated from the solution by the assistance of an external magnetic field. For quality control, blank samples without polyacrylamide functionalized Fe₃O₄ adsorbent were run simultaneously in all experiments. In addition, triplicate experiments were completed to ensure the repeatability of the adsorption capacity values [45]. The determinations of the adsorptive removal capacity were done by measuring the metal ion concentrations with atomic absorption spectroscopy (AAS) before and after the adsorption process, and then applying the following equation:

$$q_e = (C_0 - C_e) \cdot V/M \quad (8)$$

Where q_e refers to the adsorption capacity (mg/g), C_0 refers to the initial concentration of metal ion solution, C_e refers to the equilibrium concentration of metal ion solution, V refers to the volume of the metal ion solution, and M refers to the mass of the adsorbent (g).

4. Conclusions

In this work, a one-step synthesis process was implemented simultaneously for developing a carbon coating layer together with imparting polyacrylamide functionalization for Fe₃O₄ nanoparticles using the hydrothermal technique. TEM observation indicates that the carbon coating matrix surrounding the magnetic Fe₃O₄ nanoparticles was homogeneously distributed within the matrix. FTIR spectra indicated the presence of amide I and II groups, which suggests the polyacrylamide functionalization for carbon coated Fe₃O₄. The polyacrylamide functionalized Fe₃O₄ nanoparticles produced showed resistance to leaching in an acidic medium due to protection by the carbon layer. The ability of the Fe₃O₄ nanoparticles to adsorb heavy metals was improved through functionalization with a polyacrylamide layer. As the adsorptive removal process parameters were optimized, the pseudo-second-order kinetic model was more suitable to describe the process. The adsorption data were well fitted by Langmuir and Freundlich isotherms. The thermodynamic parameters, including Gibbs free energy (ΔG°), enthalpy (ΔH°), and entropy (ΔS°), were investigated, and the results suggested spontaneous behavior for the heavy metal cations adsorption using polyacrylamide functionalized Fe₃O₄.

nanoparticles. Hence, the prepared adsorbent is recommended for separation and removal of heavy metals from wastewater by the adsorption process.

Supplementary Materials: Supplementary materials are available online.

Acknowledgments: The authors would like to extend their sincere appreciation to the Deanship of Scientific Research at King Saud University for funding this work through Research Group No. RG-1435-002.

Author Contributions: M.A.H., A.M.E.-T. and Z.A.A. conceived and designed the experiments; M.A.H., A.M.E.-T., H.E.E. performed the experiments M.A.H., A.M.E.-T. and Z.A.A. analyzed the data; J.P.L., A.K. and A.A.-M. Contributed reagents/materials/analysis tools; M.A.H. and A.M.E.-T. wrote the paper.

Conflicts of Interest: The authors declare no conflict of interest.

References

1. Bailey, S.E.; Olin, T.J.; Bricka, R.M.; Adriana, D.D.; Brickab, R.M. A review of potentially low-cost sorbents for heavy metals. *Water Res.* **1999**, *33*, 2469–2479.
2. Mehmet, E.A.; Sukru, D.; Celalettin, O.; Mustafa, K. Heavy metal adsorption by modified oak sawdust. *J. Hazard. Mater.* **2007**, *141*, 77–85.
3. Volesky, B. Detoxification of metal-bearing effluents: Biosorption for the next century. *Hydrometallurgy* **2001**, *59*, 203–216.
4. Palanisamy, K.; Nomanbhay, S.M. Removal of heavy metal from industrial wastewater using chitosan coated oil palm shell charcoal. *Electron. J. Biotechnol.* **2005**, *8*, 43–53.
5. Bódalo-Santoyo, A.; Gómez-Carrasco, J.L.; Gómez-Gómez, E.; Hidalgo-Montesinos, A.M.; Máximo-Martín, F. Application of reverse osmosis to reduce pollutants present in industrial wastewater. *Desalination* **2003**, *155*, 101–108.
6. Walsh, F.C.; Reade, G.W. Electrochemical techniques for the treatment of dilute metal-ion solutions. *Stud. Environ. Sci.* **1994**, *59*, 3–44.
7. Xing, Y.; Chen, X.; Wang, D. Electrically regenerated ion exchange for removal and recovery of Cr(VI) from wastewater. *Environ. Sci. Technol.* **2007**, *41*, 1439–1443.
8. Srivastava, V.; Weng, C.H.; Singh, V.K.; Sharma, Y.C. Adsorption of nickel ions from aqueous solutions by nano alumina: Kinetic, mass transfer, and equilibrium studies. *Chem. Eng. Data* **2011**, *56*, 1414–1422.
9. AlOthman, Z.A.; Habila, M.A.; Hashem, A. Removal of zinc(II) from aqueous solutions using modified agricultural wastes: Kinetics and equilibrium studies. *Arab. J. Geosci.* **2012**, *6*, 4245–4255.
10. Repo, E.; Warchol, J.K.; Bhatnagar, A.; Mudhoo, A.; Sillanpää, M. Aminopolycarboxylic acid functionalized adsorbents for heavy metals removal from water. *Water Res.* **2013**, *47*, 4812–4832.
11. Srivastava, S.K.; Gupta, V.K.; Mohen, D. Removal of lead and chromium by activated slag—A blast-furnace waste. *J. Environ. Eng.* **1997**, *123*, 461–468.
12. Al-Ashesh, S.; Banat, F.; Al-Omari, R.; Duvnjak, Z. Predictions of binary sorption isotherms for the sorption of heavy metals by pine bark using single isotherm data. *Chemosphere* **2000**, *41*, 659–665.
13. AlOthman, Z.A.; Hashem, A.; Habila, M.A. Kinetic, equilibrium and thermodynamic studies of cadmium (II) adsorption by modified agricultural wastes. *Molecules* **2011**, *16*, 10443–10456.
14. Wang, X.; Guo, Y.; Yang, L.; Cheng, X.; Zhao, J.; Han, M. Nanomaterials as Sorbents to Remove Heavy Metal Ions in Wastewater Treatment. *J. Environ. Anal. Toxicol.* **2012**, *2*, 1–7.
15. Nata, I.F.; Salim, G.W.; Lee, C. Facile preparation of magnetic carbonaceous nanoparticles for Pb²⁺ ions removal. *J. Hazard. Mater.* **2010**, *183*, 853–858.
16. Zhu, L.; Ma, J.; Jia, N.; Zhao, Y.; Shen, H. Chitosan-coated magnetic nanoparticles as carriers of 5-fluorouracil: Preparation, characterization and cytotoxicity studies. *Colloids Surf. B Biointerfaces* **2009**, *68*, 1–6.
17. Morales, M.A.; Mascarenhas, A.J.S.; Gomes, A.M.S.; Galembeck, F.; Leite, C.A.P.; Andrade, H.M.C.; de Castilho, C.M.C. Synthesis and characterization of magnetic mesoporous particles. *J. Colloid Interface Sci.* **2010**, *342*, 269–277.
18. Deng, Y.H.; Cai, Y.; Sun, Z.K.; Zhao, D. Magnetically responsive ordered mesoporous materials: A burgeoning family of functional composite nanomaterials. *Chem. Phys. Lett.* **2011**, *510*, 1–13.
19. Martínez-Cabanás, M.; López-García, M.; Barriada, J.L.; Herrero, R.; Manuel, E.; de Vicente, S. Green synthesis of iron oxide nanoparticles. Development of magnetic hybrid materials for efficient As(V) removal. *Chem. Eng. J.* **2016**, *301*, 83–91.

20. Liu, H.; Li, Z.; Takafuji, M.; Ihara, H.; Qiu, H. Octadecylimidazolium ionic liquid-modified magnetic materials: Preparation, adsorption evaluation and their excellent application for honey and cinnamon. *Food Chem.* **2017**, *229*, 208–214.
21. Cheng, Z.; Li, Y.; Liu, Y. Novel adsorption materials based on graphene oxide/Beta zeolite composite materials and their adsorption performance for rhodamine B. *J. Alloys Compd.* **2017**, *708*, 255–263.
22. Schneider, S.J. *Engineered Materials Handbook: Ceramics and Glasses*; ASM International: Materials Park, OH, USA, 1991.
23. Hao, Y.M.; Chen, M.; Hu, Z.B. Effective removal of Cu(II) ions from aqueous solution by amino-functionalized magnetic nanoparticles. *J. Hazard. Mater.* **2010**, *184*, 392–399.
24. Wang, J.H.; Zheng, S.R.; Shao, Y. Amino-functionalized Fe₃O₄@SiO₂ core-shell magnetic nanomaterial as a novel adsorbent for aqueous heavy metals removal. *J. Colloid Interface Sci.* **2010**, *349*, 293–299.
25. Pang, Y.; Zeng, G.M.; Tang, L.Y.; Xie, G.; Li, Z.; Zhang, J. PEI-grafted magnetic porous powder for highly effective adsorption of heavy metal ions. *Desalination* **2011**, *281*, 278–284.
26. Peng, X.H.; Wang, Y.J.; Tang, X.L.; Liu, W. Functionalized magnetic core-shell Fe₃O₄@SiO₂ nanoparticles as selectivity-enhanced chemosensor for Hg(II). *Dyes Pig.* **2011**, *91*, 26–32.
27. Zhang, M.; Zhang, Z.; Liu, Y.; Yang, X.; Luo, L.; Chen, J.; Yao, S. Preparation of core-shell magnetic ion-imprinted polymer for selective extraction of Pb(II) from environmental samples. *Chem. Eng. J.* **2011**, *178*, 443–450.
28. Mahmoud, M.E.; Abdelwahab, M.; Fathallah, E.M. Design of novel nano-sorbents based on nano-magnetic iron oxide-bound-nano-siliconoxide-immobilized-triethylenetetramine for implementation in water treatment of heavy metals. *Chem. Eng. J.* **2013**, *223*, 318–327.
29. Tang, Y.; Liang, S.; Yu, S.; Gao, N.; Zhang, J.; Guo, H.; Wang, Y. Enhanced adsorption of humic acid on amine functionalized magnetic mesoporous composite microspheres. *Colloids Surf. A Physicochem. Eng. Asp.* **2012**, *406*, 61–67.
30. Tang, Y.; Liang, S.; Wang, J.; Yu, S.; Wang, Y. Amino-functionalized core-shell magnetic mesoporous composite microspheres for Pb(II) and Cd(II) removal. *J. Environ. Sci.* **2013**, *25*, 830–837.
31. Itoh, H.; Sugimoto, T. Systematic control of size, shape, structure, and magnetic properties of uniform magnetite and maghemite particles. *J. Colloid Interface Sci.* **2003**, *265*, 283–295.
32. Huang, X.; Wang, G.; Yang, M.; Guo, W.; Gao, H. Synthesis of polyaniline modified Fe₃O₄/SiO₂/TiO₂ composite microsphere and photocatalytic application. *Mater. Lett.* **2011**, *65*, 2887–2890.
33. You, L.J.; Xu, S.; Ma, W.F.; Li, D.; Zhang, Y.T.; Guo, J.; Hu, J.J.; Wang, C.C. Ultrafast hydrothermal synthesis of high quality magnetic core phenol–Formaldehyde shell composite microspheres using the microwave method. *Langmuir* **2012**, *28*, 10565–10572.
34. Ayub, S.; Ali, S.I.; Khan, N.A. Study on the removal of Cr(VI) by sugarcane bagasse from wastewater. *Pollut. Res. J.* **2001**, *2*, 233–237.
35. Hashem, A.; Abdel-Halim, E.S.; El-Tahlawy, K.F.; Hebeish, A. Enhancement of the adsorption of Co(II) and Ni(II) ions onto peanut hulls through esterification using citric acid. *Adsorpt. Sci. Technol.* **2005**, *23*, 367–380.
36. Wen, D.; Ho, V.Y.S.; Tang, X. Comparative sorption kinetic studies of ammonium onto zeolite. *J. Hazard. Mater.* **2006**, *133*, 252–256.
37. HO, Y.S.; Mckay, G.; Wase, D.A.J.; Foster, C.F. Study of the sorption of divalent metal ions on to peat. *Adsorpt. Sci. Technol.* **2000**, *18*, 639–650.
38. Mohan, D.; Gupta, V.K.; Srivastava, S.K.; Chander, S. Kinetics of mercury adsorption from wastewater using activated carbon derived from fertilizer waste. *Colloids Surf. A* **2001**, *177*, 169–181.
39. Najafi, M.; Rostamian, R.; Rafati, A.A. Chemically modified silica gel with thiol group as an adsorbent for retention of some toxic soft metal ions from water and industrial effluent. *Chem. Eng. J.* **2011**, *168*, 426–432.
40. Chang, S.T.; Chang, H.T. Comparisons of the photostability of esterified wood. *Polym. Degrad. Stab.* **2001**, *71*, 261–266.
41. Tjeerdsma, B.F.; Militz, H. Chemical changes in hydrothermal treated wood: FTIR analysis of combined hydrothermal and dry heat-treated wood. *Eur. J. Wood Wood Prod.* **2005**, *63*, 102–111.
42. Horsfall, M.; Spiff, A.I.; Abia, A.A. Studies on the influence of mercaptoacetic acid (MAA) modification of cassava (*Manihotesculentacranz*) waste Biomass on the adsorption of Cu²⁺ and Cd²⁺ from aqueous solution. *Bull. Korean Chem. Soc.* **2004**, *25*, 969–976.

43. Malkoc, E.; Nuhoglu, Y. Determination of kinetic and equilibrium parameters of the batch adsorption Cr(IV) onto waste acorn of *Quercusithaburensis*. *Chem. Eng. J.* **2007**, *46*, 1020–1029.
44. Wang, Y.; Tang, X.; Chen, Y.; Zhan, L.; Li, Z.; Tang, Q. Adsorption behavior and mechanism of Cd(II) on loess soil from China. *J. Hazard. Mater.* **2009**, *172*, 30–37.
45. Azizi, S.; Kamika, I.; Tekere, M. Evaluation of heavy metal removal from wastewater in a modified packed bed biofilm reactor. *PLoS ONE* **2016**, *11*, 1–13.

Sample Availability: Samples of the compounds polyacrylamide functionalized Fe₃O₄ nanoparticles are available from the authors.



© 2017 by the authors. Licensee MDPI, Basel, Switzerland. This article is an open access article distributed under the terms and conditions of the Creative Commons Attribution (CC BY) license (<http://creativecommons.org/licenses/by/4.0/>).